SEAM SMOOTHING OF DIGITAL COLOR MOSAICS

Hao-Hsiung Huang
Associate Professor

Department of Surveying and Mapping Engineering
Chung Cheng Institute of Technology
Tahsi, Taoyuan, 335 Taiwan, Republic of China
Commission IV

ABSTRACT:

The discontinuous tone and unavoidable seam between photos due to image mismatching can usually be detected on a traditional controlled mosaic. To minimize this detectable effects and establish an efficient digital mosaic system is thus the purpose of this paper. Polynomial fitting technique has been used to define seams which are then eliminated by the use of smoothing.

The system was tested by producing two controlled mosaics from two blocks of color images respectively, taken under various photo distances and illuminations by the use of a CCD camera. These two mosaics were found to be of high compatibility.

KEY WORDS: Digital Mosaics, Seam Smoothing, Image Processing

1. INTRODUCTION

Traditionally, the discontinuous tone and unavoidable seam between photos due to image mismatching can easily be visualized when two or more images of a scene are mosaicked. The computer methods for digital mosaics would minimize the degree of mismatch (Milgram, 1975; 1977).

Most papers concerned with mosaics discussed images acquired by satellite. Very few authors have covered digital mosaics using a set of pictures taken by a CCD camera. Various factors intervene to make the mosaicking of CCD images difficult (Jensen, 1986). Cameras uncertainty and lens distortion can cause registration error.

However, digital images can be obtained quickly and cheaply by using a CCD camera. It is thus worth studying how to rectify CCD images and combine them together.

As described by Milgram (1977), images were registered respectively firstly, gray-levels of two adjacent images were then equalized, and seam was defined and smoothed finally. In this paper, the author uses similar procedures and additionally presents a simple method that makes tone vary continuously from one image to the next. Seam is also defined as a polynomial curve, and so smoothed that the final mosaic looks like a single image.

2. RECTIFICATION

Resampling technology is used to rectify the deformed images. Any of three resampling methods, nearest neighbor, bilinear interpolation, and bicubic interpolation can usually be adopted (Lillesand and Kiefer, 1987). Since bicubic interpolation gives the best image quality, it has therefore been used throughout in this study.

Three rectification methods, polynomial rectification, projective transformation, and differential rectification are commonly used in image processing systems (Novak, 1992). Two-dimensional projective transformation equations can complete the analytical rectification of a tilted image (Wolf, 1983). Since a CCD camera as used in this study, usually takes a tilted image. Equations as shown below, of a two-dimensional projective transformation were thus applied for rectification.

$$X = \frac{a_1 x + b_1 y + c_1}{a_3 x + b_3 y + 1}$$
$$Y = \frac{a_2 x + b_2 y + c_2}{a_3 x + b_3 y + 1} \tag{1}$$

Where
a_1, a_2, a_3, b_1, b_2, b_3, c_1, c_2 are the transformation parameters,
X, Y are coordinates of the original image, and
x, y are coordinates of the registered image.

More than four control points are required to obtain a least squares solution for the parameters in Eqs. (1).

3. TONE CONTINUOUS

Let L be the left image and R be the right image. These two images have been registered respectively and have to be mosaicked. Two histograms of their respective overlap areas, O_l and O_r would be ideally identical. But various illuminative conditions affect the histograms differentially. Hord (1982) mentioned that the gray-levels of the two images could be so stretched that the average gray-levels, μ_l of O_l matched the average gray-levels, μ_r of O_r.

Let σ_l and σ_r be the standard deviations of gray-levels of O_l and O_r respectively. When the L and the R images were been processing, the following equations could be used to improve the Hord's method.

$$G_l' = \frac{G_l - \mu_l}{\sigma_l}\sigma + \mu$$
$$G_r' = \frac{G_r - \mu_r}{\sigma_r}\sigma + \mu \tag{2}$$

Where

$$\mu = (\mu_l + \mu_r)/2 \qquad (3)$$
$$\sigma = (\sigma_l + \sigma_r)/2$$

G_l and G_r are the input gray-levels of the left and right images respectively, and
G_l' and G_r' are the output gray-levels of the left and right images respectively.

Owing to light falloff problem, global adjustment method as just described, will not eliminate significant artificial edges. One can expect that this degree of appearence can be decreased by processing on a row by row basis. Let $\Delta_1, \Delta_2, \ldots, \Delta_m$, be the differences of average gray-levels for each row in O_l and O_r. Here,

$$\Delta_i = \sum_{j=1}^{n} (L_{ij} - R_{ij})/n \qquad (4)$$

O_l and O_r have the same sizes of m rows by n columns. In general, the Δ's could be assumed vary continuously from one row to the next. Therefore, they would be fitted using a polynomial transformation equation as expressed below.

$$\Delta_i = a_0 + a_1 i + a_2 i^2 + a_3 i^3 + \ldots \qquad (5)$$

When equations of the type of Eq.(5) have been written for all rows, a least squares solution can be obtained for the parameters in Eq.(5). These parameters are then used in Eq.(5) to compute the regressive values of the Δ's for each row.

The new $\Delta_i/2$ values are then subtracted to each pixel of the corresponding row on the left image, and added to each pixel of the corresponding row on the right images. The resultant images can be prepared for the "seam definition and smoothing" step as described below.

4. SEAM DEFINITION AND SMOOTHING

As stated by Milgram and Hord, a seam point for each row can be defined by the following equation.

$$D_j = \sum_{k=-w/2+1}^{w/2} | L_{j+k} - R_{j+k} | \qquad (6)$$

Where D_j are the sums of differences over w pixels, and j would be found when D_j is minimal. The seam point would then be located at pixel j on the current row.

However, horizontal positions of a succession of seam points obtained by this method are unrelated to each other. This usually causes horizontal artificial edges on the mosaics. In avoiding this appearance, one can restrict that the seam points positions, j vary continuously from one row to the next. Again, a polynomial transformation equation similar to Eq.(5) would be applied, and j is substituted for Δ, as follows:

$$j_i = a_0 + a_1 i + a_2 i^2 + a_3 i^3 + \ldots \qquad (7)$$

A type of Eq.(7) can be written for each row, and m equations may be formed containing the four unknown parameters. The equations are solved by the method of least squares to obtain the most probable transformation parameters. These parameters are then used in Eq.(7) to compute the adjusted values of the j'_s for each row.

Once a seam point has been determined, the image information in the mosaic to the left of the seam point will come from the line segment of image L, and the information to the right from the the image R. Fig.1 shows gray-levels of sample overlapping windows.

The smoothing of the gray-levels changed at each of the seam points is the final step. A ramp function expressed by Milgram (1975) may be adopted.

5. EXPERIMENT

A colorful original was chosen in this study. Thirty grided targets were marked on the original, and were used for control points. Two blocks of color images respectively, using red, green, and blue filters individually, were taken under various photo distances and illuminations by the use of a CCD camera. One block was composed of two pictures as shown in Fig.2, and the other one was composed of three pictures as shown in Fig.3.

Image coordinates of control points on each of five pictures were then measured. These coordinates (X, Y) and their corresponding theoretical coordinates (x, y) on the rectified images were used to compute the transformation parameters. Each of the original images was then registered by the use of these parameters and resampling technology.

Two controlled mosaics were then produced respectively, using the process indicated previously. The first mosaic shown in Fig.4, was generated from two registered images. The second one shown in Fig.5, was generated from three registered images. The difference of two mosaics was processed and shown in Fig.6. The two mosaics are found to be of high compatibility. A seam curve is also visible in Fig.6.

6. CONCLUSIONS

Based upon the results of this study, several conclusions can be drawn, as follows:

(1)The accuracy of geometric registration strongly influences the quality of a mosaic. In order to successfully mosaick the adjacent images, the method of the geometric transformations must be considered. A two-dimensional projective transformation used in this study is good enough for registration of the images on two non-parallel planes.

(2)Tone continuous processing of the adjacent images results in enhancing the effect of a smooth transition across the seam. The seam points positions can thus vary continuously, as expected, from one row to the next.

(3)Cameras uncertainty and lens distortion may introduce geometric errors of an image. Investigation on eliminating these errors should be considered.

(4)The polynomial fitting model was used in two aspects, tone change and seam points change from one row to the next. Further study of using another model would be desirable.

REFERENCE

Hord, R.M., 1982. Digital Image Processing of Remotely Sensed Data. Academic Press, Inc., New York, pp.72-74.

Jensen, J.R., 1986. Introductory Digital Image Processing. Prentice-Hall, New Jersey, p.16.

Kunji, B., 1985. Experiments in Digital Processing of Photogrammetric Data. ITC Journal, 1985-1.

Lillesand, T.M., and R.W. Kiefer, 1987. Remote Sensing and Image Interpretation. John Wiley & Sons, Inc., New York, pp.612-616.

Milgram, D.L., 1975. Computer Methods for Creating Photomosaics. IEEE Transactions on Computers, Vol. C-24, pp.1113-1119.

Milgram, D.L., 1977. Adaptive Techniques for Photomosaics. IEEE Transactions on Computers, Vol. C-26, pp.1175-1180.

Novak, K., 1992. Rectification of Digital Imagery. Photogrammetric Engineering and Remote Sensing, Vol.58, No.3, pp.339-344.

Sabins, F.F., 1987. Remote Sensing Principles and Interpretation. W.H. Freeman and Company, New York, p.259.

Wolf, P.R., 1983. Elements of Photogrammetry. 2nd ed., McGrawHill Book Co., Inc., New York, pp.211-212.

Zobrist, A.L., N.A. Bryant, and R.G. McLeod, 1983. Technology for Large Digital Mosaics of Landsat Data. Photogrammetric Engineering and Remote Sensing, Vol.49, No.9, pp.1325-1335.

130	127	139	133	145	135	<u>138</u>	142	142	124	146	138	136	140	135
129	135	137	136	125	142	145	<u>143</u>	157	126	136	135	133	143	133
137	158	135	135	123	141	152	<u>137</u>	148	145	124	126	147	140	136

(a) Left image.

139	156	149	134	126	140	<u>125</u>	124	132	134	145	135	136	124	131
142	152	135	133	127	147	140	<u>129</u>	132	140	129	133	140	121	129
145	141	129	139	134	129	133	<u>133</u>	144	145	136	138	139	136	115

(b) Right image.

132	129	141	135	147	137	<u>131</u>	122	130	132	143	133	134	122	129
131	137	139	138	127	144	147	<u>136</u>	130	138	127	131	138	119	127
139	160	137	137	125	143	154	<u>135</u>	142	143	134	136	137	134	113

(c) Mosaics.

Figure 1. Gray-levels of sample overlapping windows. The <u>underlined</u> values locate seam points.

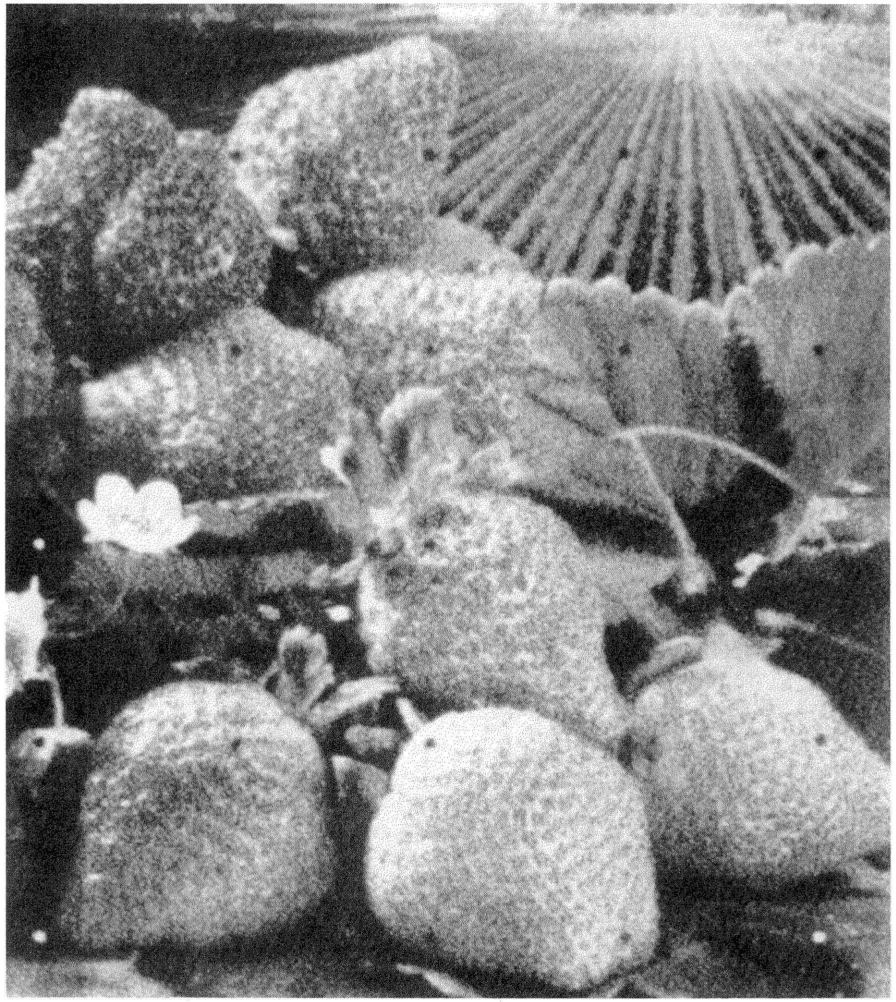

Figure 2. Two registered images. Seam is visible.

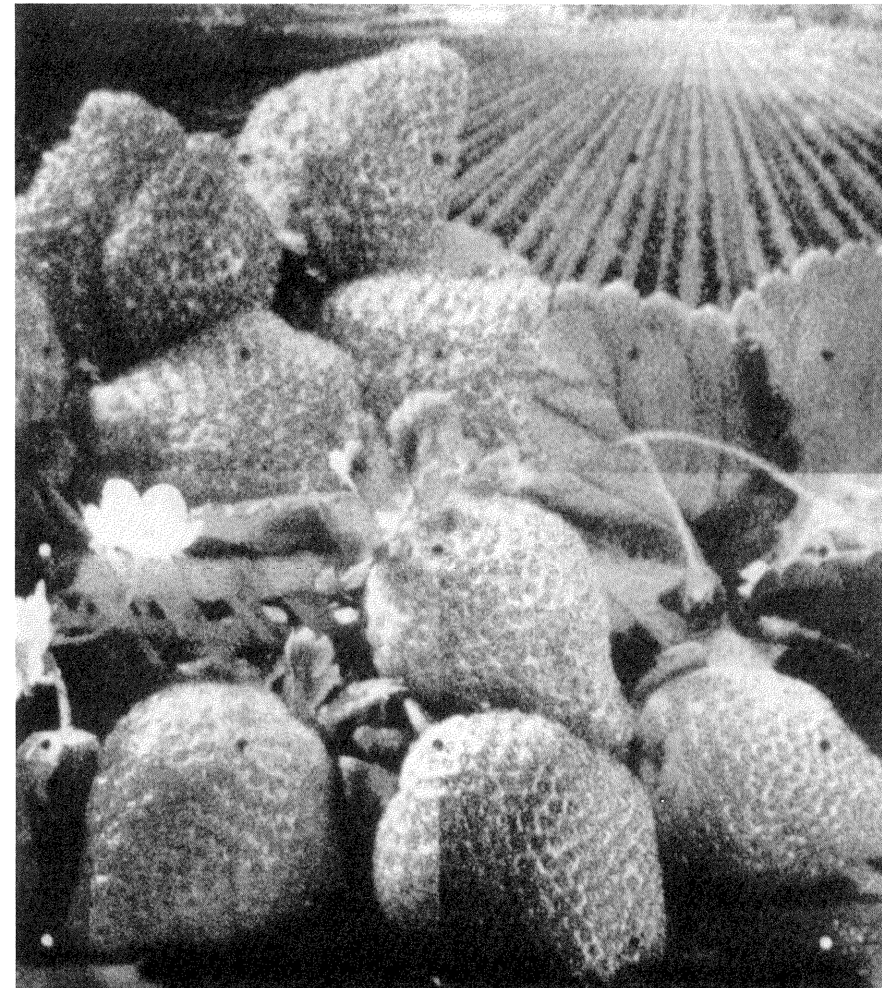

Figure 3. Three registered images. Seam is visible.

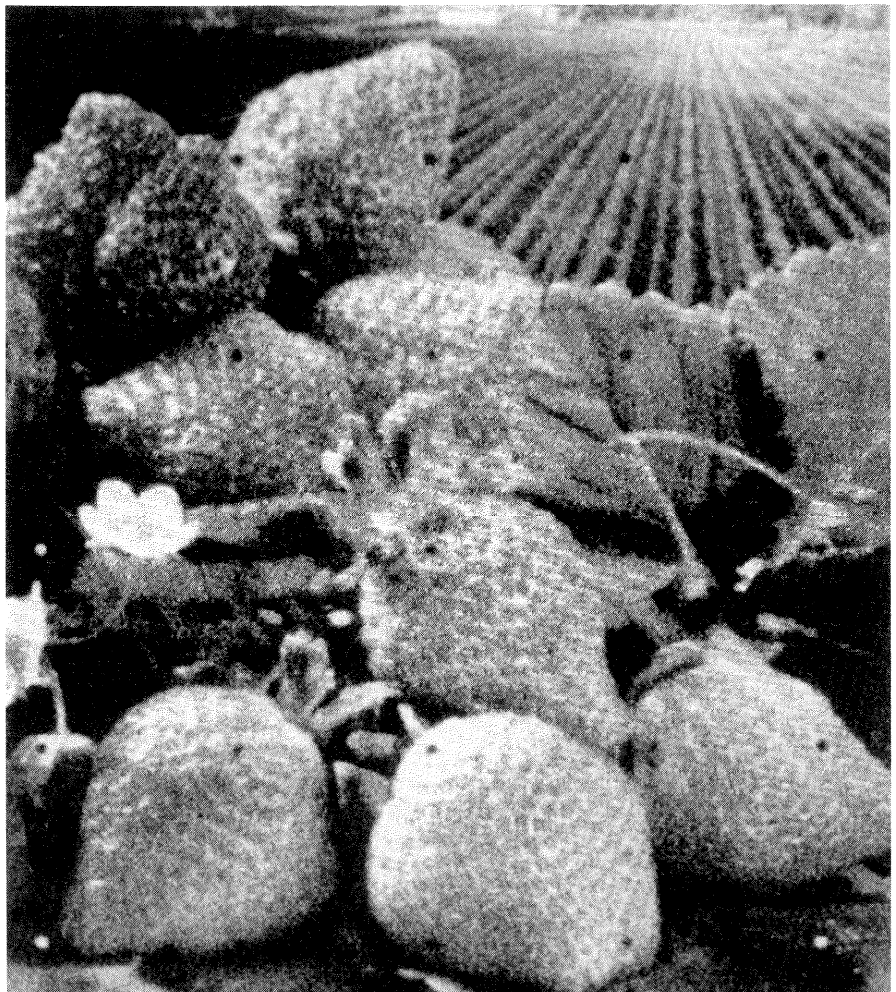

Figure 4. Mosaic of Fig.2.

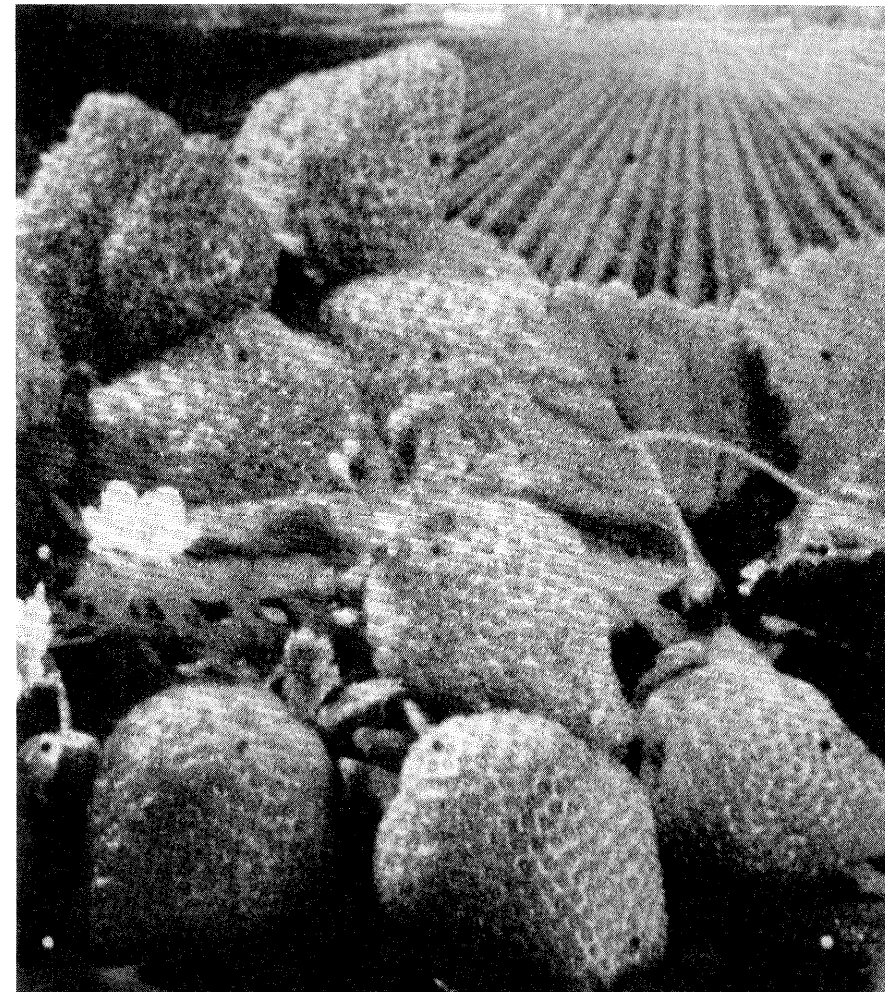

Figure 5. Mosaic of Fig.3.

Figure 6. Difference of Figs.4 and 5,
with seam curve made visible.